Electronic Coherence and Collective Optical Excitations of Conjugated Molecules

Shaul Mukamel *, Sergei Tretiak, Thomas Wagersreiter, and Vladimir Chernyak

Optical spectroscopy of conjugated molecules is described by using collective electronic coordinates, which represent the joint dynamics of electron-hole pairs. The approach relates the optical signals directly to the dynamics of charges and bond orders (electronic coherences) induced by the radiation field, and uses only ground state information, thus totally avoiding the explicit calculation of excited molecular states. The resulting real-space picture is reminiscent of the normal mode analysis of molecular vibrations and offers a unified framework for the treatment of other types of systems including semiconductor nanostructures and biological complexes. Spatial coherence displayed in two-dimensional plots of the five electronic normal modes which dominate the optical response of Poly(p-phenylene vinylene) (PPV) oligomers with up to 50 repeat units (398 carbon atoms) in the 1.5 to 8 eV frequency range suggests a saturation to bulk behavior at about 5 repeat units.

Spectroscopy allows chemists and physicists to probe of the dynamics of vibrations and electronic excitations within molecules and solids. The theoretical models used for interpreting molecular spectra versus those for extended solids are usually quite different, and certain systems, such as clusters and polymers, are not readily treated by either of these limiting cases. We are espesially interested in understanding the optical spectra of large polymers, which are extended conjugated molecules such as poly(p-phenylene vinylene) oligomers (Fig. 1) that have interesting optical applications.

Electronic and optical properties of small conjugated chains can be interpreted molecularly in terms of their global many-electron eigenstates obtained from quantum-chemistry methods [1,2]. Large polymers can also be treated by using semiconductor band theories that focus on the dynamics of electron-hole pairs [3]. The size-scaling of the optical response, and the transition between these two regimes has not been fully explored for the lack of adequate theoretical methods. The eigenstates, which carry considerably more information than necessary for the calculation of spectra, are hard to get

The authors are in the Department of Chemistry and the Rochester Theory Center for Optical Science and Engineering, University of Rochester, Rochester, NY 14627, USA.

* To whom correspondence should be addressed.

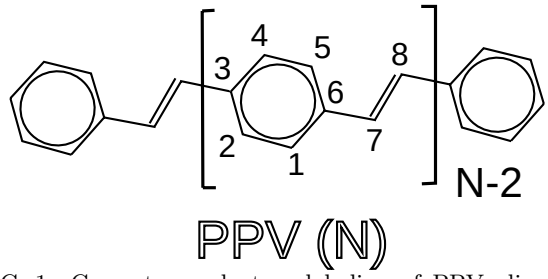

FIG. 1. Geometry and atom labeling of PPV oligomers. Bond angles are 120°, except $\alpha(r_{6,7}, r_{7,8}) = 128^o$, and the distances are: $r_{1,2} = r_{2,3} = r_{3,4} = r_{4,5} = r_{5,6} = r_{6,1} = 1.39\mathring{A}$, $r_{6,7} = 1.44\mathring{A}$, $r_{7,8} = 1.33\mathring{A}$.

for large molecules with strong electron correlations (as occurs in conjugated chains). Band theories, however, neglect electronic correlation effects, and because they are formulated in momentum (k) space they do not lend themselves very easily to real-space chemical intuition.

The collective-electronic oscillator (CEO) representation [4,5] provides a hybrid formulation that bridges the gap between the chemical and semiconductor points of view. This model uses an electron-hole picture in real-space, overcomes many of the difficulties associated with the former approaches, and provides a physically-intuitive link between electronic structure and optical properties, that is, they are related directly to the motions of charges and electronic coherences, thus avoiding the need to calculate the global (many-electron) eigenstates, which is computationally demanding and in fact overdetermines the problem. The electronic oscillators, unlike the electronic orbitals, directly represent spectroscopic observables [4–6]. Despite the quantum nature of electronic motions, the collective oscillators are classical [7,8], which connects well with chemical intuition. Typically only a few oscillators dominate the response, which greatly simplifies the theoretical description. A real space picture of linear absorption which pinpoints the origin of each optical transition is obtained by two-dimensional display of the electronic mode matrices. Our results allow the interpretation of the most interesting crossover region toward the bulk.

The CEO Approach

The oscillator picture that we use here is more familiar in the analysis of vibrational spectroscopy [9], in which the coherent motion of various atoms with well-defined amplitude and phase relations are represented by collec-

tive nuclear coordinates; the normal modes. The normal modes provide a natural coordinate system and allow an alternative classical real-space interpretation of infrared or Raman spectra [10], instead of a description in terms of transitions among specific vibrational states. The normal modes of nuclear vibrations are simply superpositions of the 3N nuclear displacements. Extending this concept to electronic motions is not straightforward, however, because spectroscopic observables are highly averaged, and following the complete many-electron dynamics is neither feasible nor desirable. For this reason, the oscillator picture is normally not used for electronic spectroscopy.

In this article we show how a CEO picture can be rigorously established for optical excitations of conjugated molecules. We demonstrate how a natural set of electronic coordinates can be constructed using the reduced single-electron density matrix [4,5,11], and how it offers tremendous conceptual as well as computational advantages. Consider a conjugated molecule described by a basis set $\{\phi_n\}$ of N atomic orbitals. (For simplicity we use in the calculations presented below the Pariser-Parr-Pople (PPP) Hamiltonian where each carbon atom has a single π orbital [6,12]. N then coincides with the number of carbon atoms.) The system can then be described by the Fermi operators c_n^+ (c_n) representing the creation (annihilation) of an electron on ϕ_n. The complete many-electron wave function representing the system's ground state will be denoted $\psi_g(\mathbf{x})$, $\mathbf{x}$ being the complete set of electronic coordinates. The reduced single-electron ground state density matrix is then defined as the expectation value [13]

$$\bar{\rho}_{nm} \equiv < \psi_g | c_n^+ c_m | \psi_g >, \tag{1}$$

(Spin indices have been omitted for brevity.) The physical significance of $\bar{\rho}$ has been recognized since the early days of quantum chemistry [14]. We first note that $\bar{\rho}$ is an N x N matrix. The density matrix carries considerably less information than the complete many-electron wave function, and is, therefore, much easier to calculate. However, this information is sufficient for calculating all optical properties and develop an intuitive physical picture of the optical response. ($\psi_g(\mathbf{x})$ allows us to calculate the expectation values of products of arbitrary numbers of c_n at c_n^+ whereas $\bar{\rho}$ only gives the binary products, which represent operators depending on a single electron, hence its name). $\bar{\rho}$ is thus the quantum analog of the single particle distribution in classical statistical mechanics [15]. The ground state density matrix $\bar{\rho}_{nm}$ may be obtained by using standard quantum chemistry packages. Its diagonal elements ($n = m$) represent the charge at the m'th atom, whereas the off-diagonal elements ($n \neq m$) reflect the strength of chemical bonding between each pairs of atoms and are known as the bond-orders. Bond-order is thus associated with a phase relation (electronic-coherence) between orbitals. The eigenvectors of $\bar{\rho}$ known as the natural orbitals provide a convenient basis set for performing configuration interaction (CI) calculations and for interpreting chemical reactivity [16,17].

When the molecule is driven by an external electric field (such as provided by a photon in a spectroscopic measurement), its wave function (and consequently, the reduced density matrix) become time-dependent. We then write $\rho(t) = \bar{\rho} + \delta\rho(t)$. The matrix elements $\delta\rho_{nm}(t)$ represent the changes induced in the density matrix by the electric field. $\delta\rho_{nn}(t)$ is the net charge induced on the n-th atom, whereas $\delta\rho_{nm}(t)$ $n \neq m$ is a dynamical bond-order representing the joint amplitude of finding an electron on atom m and a hole on atom n.

Quantum chemistry techniques which calculate properties such as polarizabilities by using the many-body wave functions rapidly become more expensive with molecular size, and are therefore limited to small molecules. Furthermore, in most practical chemical applications we need much less information than carried by the complete eigenstates. This makes it hard to develop a simple intuitive understanding of various trends. A time-dependent procedure for calculating $\delta\rho(t)$ directly can be obtained as follows: We start with the Heisenberg equation of motion for $c_n^+ c_m$. This equation will not be closed, because higher order products will show up when the time derivative is calculated. Writing equations of motion for these higher products will yield increasingly higher products. This is the famous hierarchy of many-body (classical and quantum) dynamics. To overcome this difficulty we need a truncation procedure. The simplest assumes that the many-body wave function is given by a single Slater determinant at all times, and yields the time dependent Hartree-Fock (TDHF) equations of motion [18]:

$$\delta\dot{\rho} = A\delta\rho + B\delta\rho\delta\rho - \mathcal{E}(t)\mu\delta\rho. \tag{2}$$

The coefficients in these equations are readily available and depend on the original Hamiltonian and on $\bar{\rho}$ (which is the essential input in the present approach). In Fig.2 we display $\bar{\rho}$ of a linear 30-atom polyacetylene chain as well as the induced density matrix $\delta\rho(\omega)$ (the Fourier transform of $\delta\rho(t)$) to first order in an external field, for three frequencies corresponding to the lowest peaks in the optical absorption. $\bar{\rho}$ is almost diagonal; only nearest neighbors have significant off-diagonal elements. This result is in agreement with our elementary picture of chemical bonding. Optical excitations, however, induce electronic coherences between atoms that are much farther apart, as is clearly seen in Fig. 2, B, C, and D.

Equation (2) allows us to calculate the time-dependent density matrix (and optical excitations) directly from $\bar{\rho}$. By understanding the mechanism for the creation of the coherence, we can develop a new type of chemical intuition and relate the optical response directly to the motions of charges and bond orders. This is an attractive alternative to the conventional description of spectra in terms of transitions among eigenstates. Both pictures are correct, and for historical reasons, chemical intuition

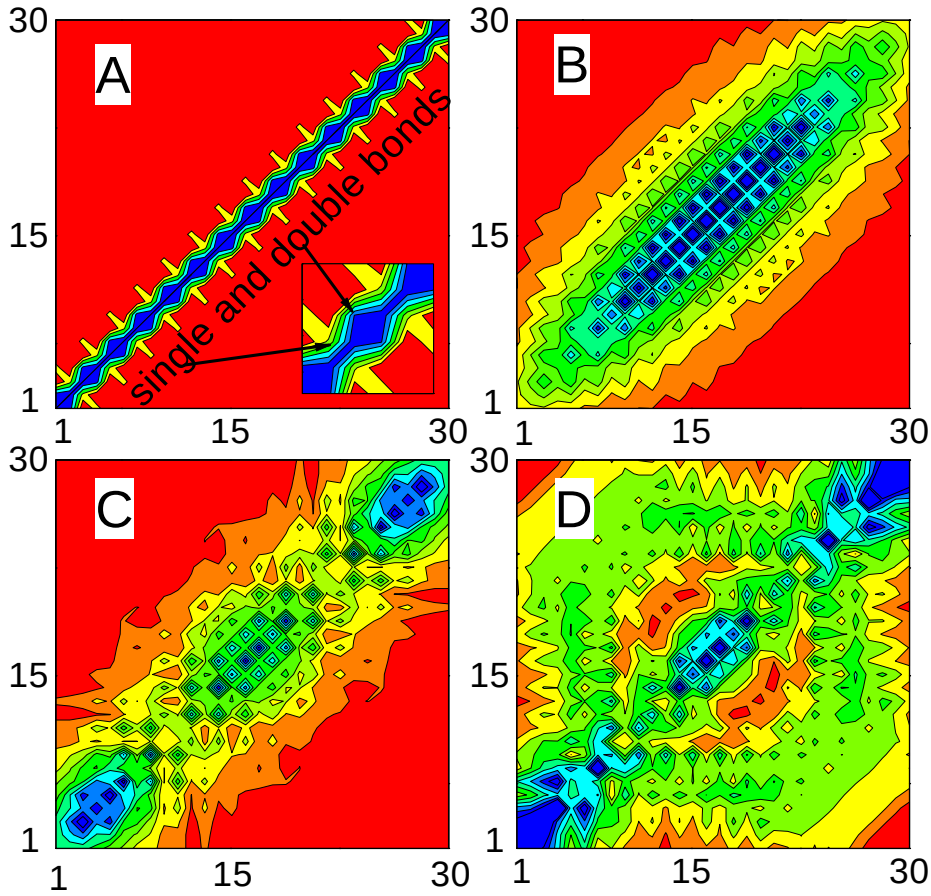

FIG. 2. Contour plots of density matrices of a 30 carbon atom polyacetylene chain: (**A**) ground state density matrix $\bar{\rho}$; (**B**), (**C**), and (**D**) frequency-dependent density matrices $\delta\rho(\omega)$ at ω =2.5, 3.5, and 4.7 eV (496, 354 and 264 nm) corresponding to the lowest three dominant peaks in the absorption spectrum. The axes represents the individual carbon atoms, and the color code is shown in Fig.4.

is traditionally based on eigenstates. However, we argue that the real-space picture is much more natural, intuitive and easier to implement once the proper terminology is developed. To illustrate this point, let us consider the variation of optical properties such as the electronic band gap and its oscillator strength or the magnitude of the off-resonant polarizability with molecular size. These properties strongly depend on size for short chains and level off at about 20 to 30 double bonds, where they attain the bulk values [19]. It is impossible to visualize this coherence size by examining the molecular orbitals. These orbitals are completely delocalized, change gradually and continuously with chain length, and contain no signatures of this coherence size. In contrast, by looking at the induced density matrix we immediately note the coherence size associated with its off-diagonal section. This coherence size which measures how far apart different atoms communicate, controls the scaling of optical properties with size, as will be demonstrated below.

At this point, we return to the analogy with classical molecular vibrations. The displacements of nuclear positions from their equilibrium values satisfy nonlinear equations of motion resulting from the anharmonic force fields. Infrared and Raman spectra are usually interpreted using normal modes obtained by diagonalizing the linear (harmonic) part of these equations of motion. Normal modes are natural collective coordinates for atomic displacements. Nonlinear (anharmonic) effects can be treated as perturbations. In complete analogy, $\delta\rho_{nm}(t)$ represent the displacements of the electronic density matrix elements from their equilibrium (ground state) values $\bar{\rho}_{nm}$. The nonlinear TDHF equations are the electronic counterpart of the classical Newtons' equations of motion of nuclear displacements. By diagonalizing the linearized TDHF equations, we obtain a set of collective electronic normal modes. The induced density matrix can then be expanded as a superposition of these collective modes in the same way that an atomic nuclear displacement is a superposition of the vibrational normal modes. Each normal mode (electronic oscillator) with frequency Ω_ν is described by a coordinate Q_ν and momentum P_ν. Q_ν and P_ν are also $N \times N$ matrices [5]. These $N^2/4$ coordinates and momenta allow us to represent the time-dependent density matrix in the form [4]:

$$\delta\rho(t) = \sum_{\nu=1}^{N^2/4} a_\nu(t)Q_\nu + b_\nu(t)P_\nu \tag{3}$$

The optical polarization is related to the charge distribution and may be expressed in terms of the diagonal elements of $\delta\rho(t)$. The polarization along the z-axis is given by:

$$< \mathcal{P}(t) >= \sum ez_n\delta\rho_{nn}(t) \tag{4}$$

where z_n is the z coordinate of the n'th atom, and e is the electronic charge.

In the CEO method [4,5], the N^2 matrix elements of $\delta\rho(t)$ are obtained by solving the closed nonlinear TDHF equations of motion [4]. These equations map the calculation of the optical response onto the dynamics of coupled electronic oscillators, (analogous to calculating molecular vibrations), thus avoiding the tedious calculation of the global (many-electron) wave functions. Infrared and Raman spectra are greatly simplified by selection rules which allow us to include only a few modes in the calculation. The same is true for the electronic normal modes: Only a few dominant modes typically determine the spectra, thus greatly simplifying the physical picture and reducing the computational effort.

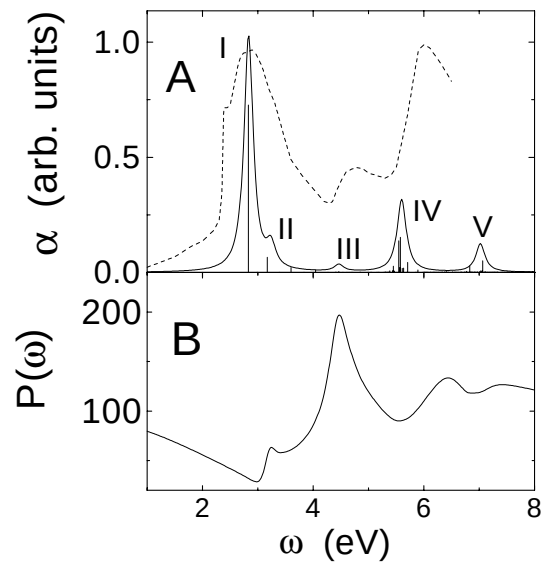

FIG. 3. (**A**) Absorption spectrum of PPV(10) (the imaginary part of α Eq.(1)). Dashed line: experimental absorption of a PPV thin film [21]. Solid line: absorption lineshape of PPV(10) obtained with 12 effective modes calculation with linewidth $\Gamma_\nu = 0.1eV$; The sticks represent oscillator strengths f_ν, $\nu = 1, N^2/4$ of PPV(10) obtained by the full TDHF. (**B**) The frequency – dependent participation ratio of the induced density matrix.

Two-Dimensional Real-Space Analysis of Optical Responses

We investigated the electronic excitations of PPV oligomers (Fig. 1) [6,20–27] and analyzed their scaling with size. Recent interest in PPV is connected with its possible use as a photoconductor [28,29], candidate for electroluminescent devices, or optical switches.

The π molecular orbitals of PPV have been classified as either localized (l) or delocalized (d) [28,26]. The former have an electron density on carbon atoms 1,2,4, and 5 (Fig.1), while the latter are delocalized over all carbon atoms. The experimental absorption spectrum of PPV thin film [21] shown in Fig.3A (dashed line) is typical for other PPV-derivatives [28,21,25]. It has a fundamental ($d \rightarrow d^\star$) band at 2.5 eV [496 nm] (I), two weak peaks at 3.7 eV [335 nm] ($d \rightarrow d^\star$) (II) and 4.8 eV [258 nm] ($l \rightarrow d^\star$ and $d \rightarrow l^\star$) (III), and a strong ($l \rightarrow l^\star$) band at 6.0 eV [207 nm] (IV). Peak II originates from electron correlations [28,26] and is missed by HF calculations. The calculated spectrum of PPV(10) shown in Fig.3A (solid line) closely resembles the experimental spectrum and has similar features at 2.83 (I), 3.3 (II), 4.5 (III), and 5.6 eV (IV) [438, 376, 276, and 221 nm]. In addition, it shows a fifth band centered at 7.0 eV [177 nm] (V). The oscillator strengths f_ν of PPV(10) are shown in Fig.3A.

By displaying the dominant oscillators in the site representation, we obtain a new picture that relates the optical properties directly to motions of charges in the system, without ever introducing electronic eigenstates. The extent of spatial coherence then provides a view of the underlying coherence sizes. A two-dimensional plot of $\bar{\rho}$ of PPV(10) is shown in Fig.4A. The coordinate axes represent repeat units along the chain and the absolute values of matrix elements are depicted by different colors. Similar to Fig. 2, $\bar{\rho}$ is dominated by the diagonal and near-diagonal elements, reflecting the bonds between nearest neighbors. Figure 4B shows a single unit of Fig. 4A on an expanded scale using the atom labeling given in Fig.1. It reflects bond strength distribution over the benzene ring (1-6 elements), strong double bond (7-8), and weaker single bond (6-7) of the vinylene group. This bonding pattern is to be expected from the molecular structure.

We next turn to examine the coordinates Q_ν and momenta P_ν of the dominant electronic oscillators. Vibrational normal modes represent coherent displacements of various atoms, and these electronic modes represent the displacements of the electronic density matrix with respect to $\bar{\rho}$. The diagonal elements reflect induced charges on various atoms, whereas the off-diagonal elements represent dynamical fluctuations of interatomic chemical bonding [4–6]. Our calculations show that the absorption is dominated by five oscillators denoted I-V. The coordinate and momentum eigenvectors of the oscillator responsible for the lowest absorption peak (I) of PPV(10) are shown in Fig. 4, C and D. The same quantities for the second oscillator corresponding to peak (II) are shown in Fig. 4, F and G. Despite the different struc-

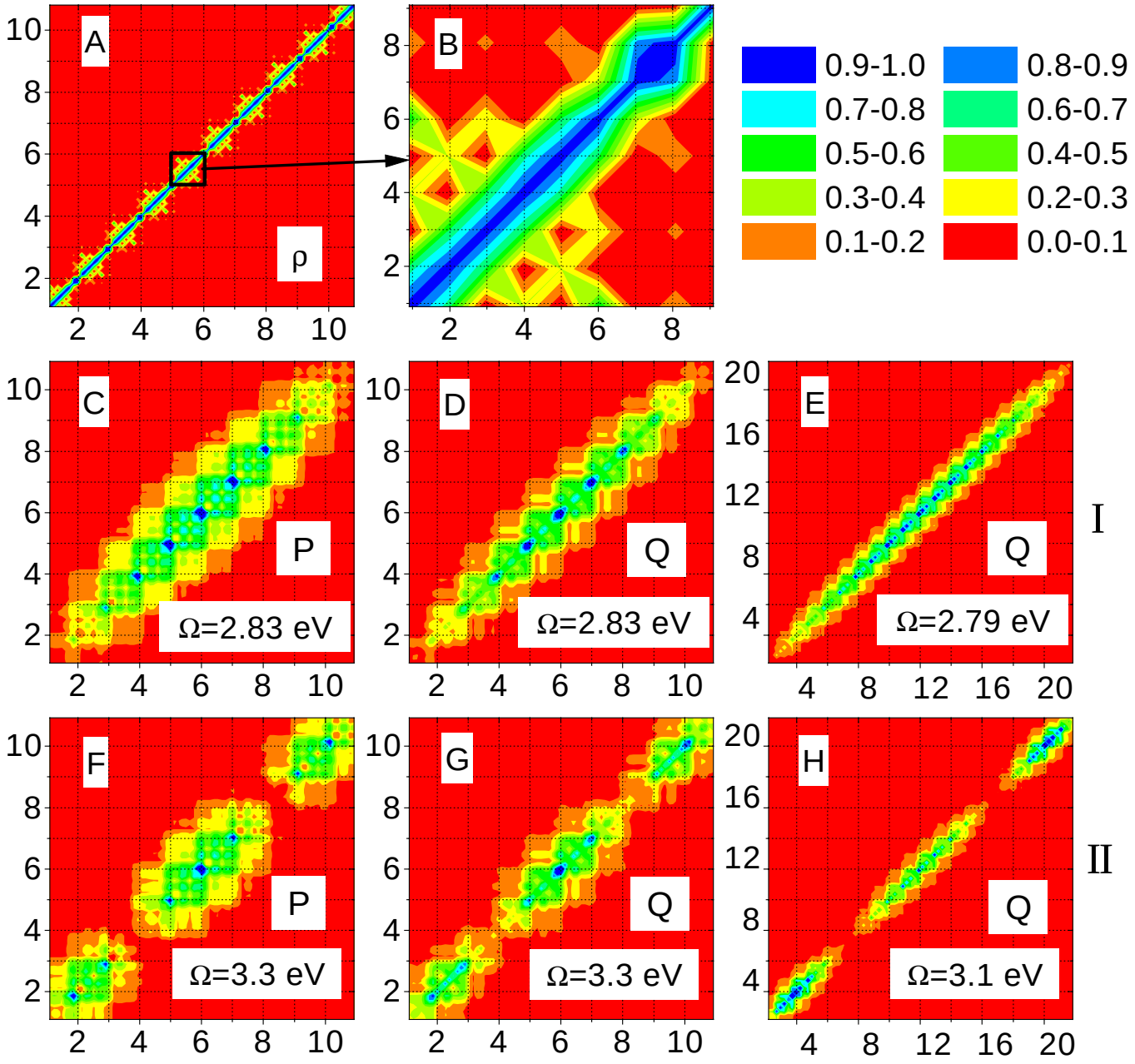

FIG. 4. Contour plots of density matrices. (**A**) $\bar{\rho}$ of PPV(10); (**B**) magnified region of (**A**) representing the single unit of polymer chain and the color maps; (**C**) momentum, and (**D**) coordinate of PPV(10), and (**E**) coordinate of PPV(20) of the lowest absorption peak (I); (**F**), (**G**), (**H**) are the same quantities as in **C** to **E** but for the second absorption peak (II). The axis labels represent the repeat units, except in (**B**) where the axes represents the individual carbon atoms as numbered in Fig.1.

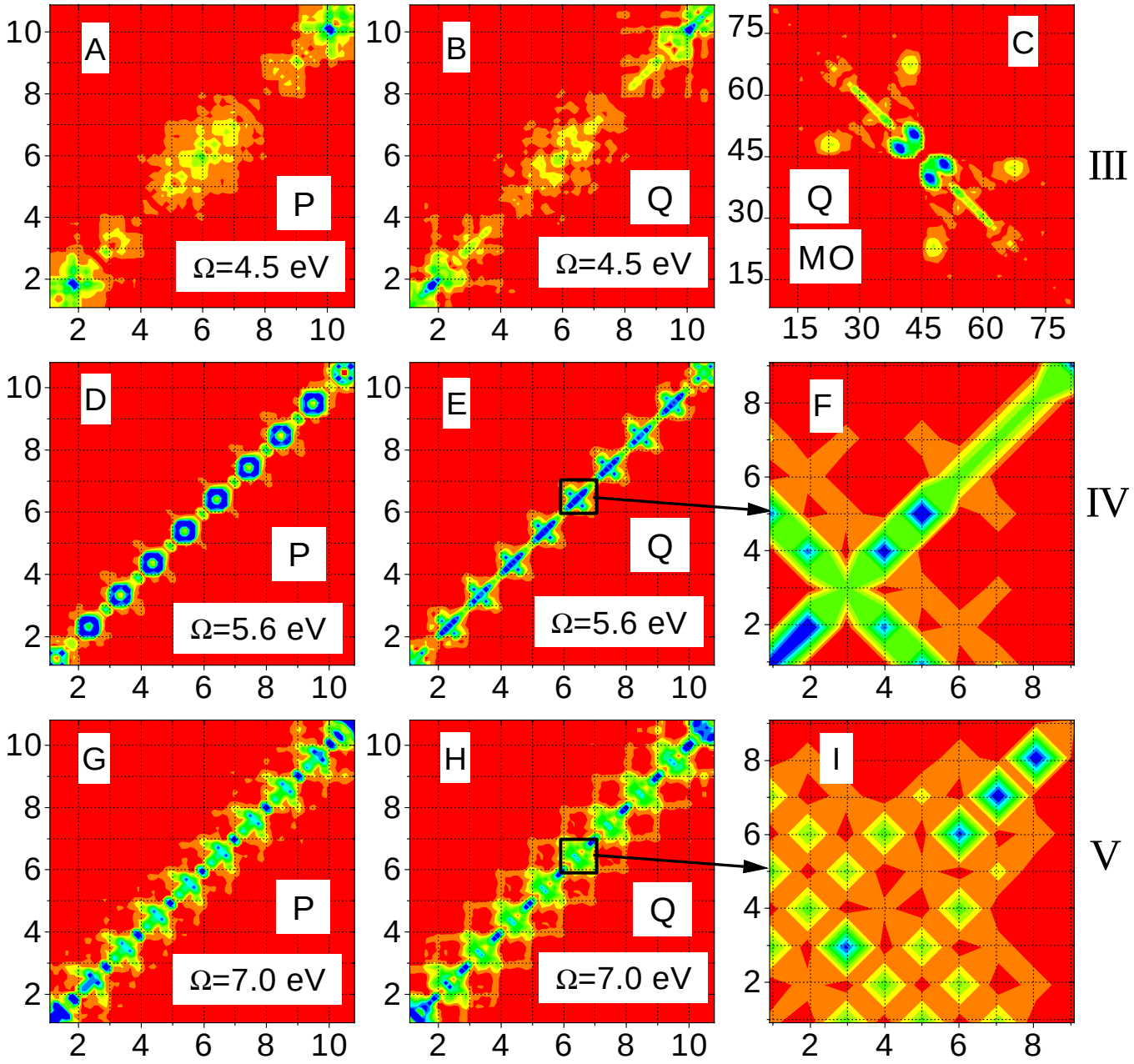

FIG. 5. Contour plots of density matrices. (**A**) Momentum, and (**B**) coordinate in the real space, and (**C**) coordinate in the molecular orbital representation of the peak (III) of PPV(10). (**D**) Momentum, and (**E**) coordinate of PPV(10) for the fourth absorption peak (IV), and (**F**) magnified area of (**E**) representing the single unit of polymer chain. (**G**, **H**, and **I**) the same quantities as in **B** to **F** but for the fifth absorption peak (V). The axis of (**A**), (**B**), (**D**), (**E**), (**G**), and (**H**) are labeled to the repeat units of polymer chain. The axis of (**C**) denote the molecular orbitals. Labeling using the number of carbon atoms according to Fig.1 is used for panels (**F**) and (**I**)

ture of these electronic modes, the delocalization pattern of the off-diagonal elements representing electronic coherence between different atoms is similar. Both modes are delocalized and can be viewed as $d \rightarrow d^\star$ transitions. Q_ν and P_ν clearly show that the weak coherences between the phenylene ring of the i-th repeat unit, and the vinylene group of the $i+1$-st repeat unit are enhanced by optical excitation. In addition, a weak dynamical coherence develops between the i-th and the $i+2$-nd repeat units. These figures illustrate that finite size effects are limited to the terminating repeat units and that the momenta are more delocalized than the coordinates for a single unit. The coherence size, that is the 'width' of the momentum density matrix along the coordinate axes, where the coherences decrease to 10% of their maximum values) is 5 repeat units. The same modes for a longer chain [(PPV(20))] displayed in Fig. 4, E and H are virtually identical to those of PPV(10). Therefore, 10 repeat units already resembles the infinite chain as far as the optical spectrum is concerned.

The coordinate and momentum of the third peak (III) of PPV(10) are shown in Fig. 5, A and B. This mode is delocalized with a coherence-size similar to modes (I) and (II), however, its structure along the oligomer chain is very different: Bonding is weak at the center and strong towards the edges. The electronic modes are most suitable for investigating charge transfer processes and photoconductivity [28,29]. The strong local optical dipoles along the chain can affect charge transfer and electron hopping. Oscillator III, which has the strongest optical coherences induced at the chain ends (see Fig. 5, A and 4, B), should play an important role in effects involving charge separation.

The coordinates and momenta of the high frequency peaks (IV) and (V) of PPV(10) (Fig. 5, D, E, G, and H) are completely localized on a single repeat unit. This behavior is drastically different from polyacetylene, where the electronic coherence-size increases monotonically for the higher frequency modes (see Fig. 2) [5]. The coordinates of these modes for a single PPV unit on an expanded scale are shown in Fig. 5, F and I. For the fourth peak (IV) the optically induced coherences only involve the phenylene ring carbon atoms 1,2,4, and 5 (Fig. 1), in agreement with the results obtained in [28,26]. The oscillator responsible for peak (IV) represents several nearly-degenerate localized oscillators (see Fig. 3A). The high-frequency peak (V) predicted by our calculations lies beyond the experimentally studied frequency range. It corresponds to localized and weakly delocalized transitions involving the vinylene group atoms 7 and 8, and the phenylene ring atoms 3 and 6. A weak coherence between the vinylene groups of neighboring repeat units is observed as well.

Even though the CEO approach is eigenstate-free, it is instructive to establish its connection to the more traditional eigenstate representation. The ν'th oscillator represents the optical transition between the ground state ψ_g and the ν'th excited state ψ_ν. The matrices representing the coordinate Q_ν and momentum P_ν are given by $(Q_\nu)_{mn} = \langle\psi_\nu|c_m^+c_n|\psi_g\rangle + \langle\psi_g|c_m^+c_n|\psi_\nu\rangle$, and $(P_\nu)_{mn} = \langle\psi_\nu|c_m^+c_n|\psi_g\rangle - \langle\psi_g|c_m^+c_n|\psi_\nu\rangle$. Q_ν and P_ν thus carry considerably reduced information about the global eigenstates $|\psi_\nu\rangle$. A different perspective on these modes is obtained by expanding them in the molecular orbital representation using a basis set of pairs molecular orbitals. Let us denote the creation (annihilation) operator for i'th molecular orbital $c_i^+(c_i)$. We then have

$$Q_\nu = \sum_{i,j}^{N^2/4} \alpha_{i,j}^\nu (c_i^+c_j + c_j^+c_i), \tag{5}$$

where i runs over initially unoccupied orbitals (particles) whereas j denotes occupied orbitals (holes) (see Fig.6A). These coefficients, normalized as $\sum_{i,j}|\alpha_{i,j}^\nu| = 1$, represent the contribution of the $j \rightarrow i$ transition to the ν'th oscillator. Note that the indices n, m used earlier represent localized atomic orbitals whereas i, j denote delocalized molecular orbitals. To illustrate how various molecular orbitals contribute to our five dominant electronic modes, we have introduced the following two quantities

$$R^\nu(j) = \sum_i [\alpha_{i,j}^\nu]^2, \;\; P^\nu = \frac{1}{\sum_{i,j}[\alpha_{i,j}^\nu]^2}, \tag{6}$$

where $i, j = 1, \ldots, N/2$, and $\nu = I, II, \ldots, V$. $R^\nu(j)$ represents the total contribution of the j'th molecular orbital to all orbital pairs appearing in the ν'th oscillator. $R^\nu(j)$ for the five dominant oscillators in PPV(10) are displayed in Fig.6B. $R^I(j)$ is relatively localized in the vicinity of the HOMO-LUMO transition (between the highest occupied and lowest unoccupied orbitals), whereas additional pairs of orbitals contribute to the higher modes. The inverse participation ratio P^ν measures the number of orbital pairs that contribute significantly to the ν'th oscillator. In the absence of electronic correlations, each oscillator represents a single transition between an occupied and an unoccupied orbitals (in the quantum chemistry terminology) or a single particle-hole pair (in the semiconductor terminology) and $P^\nu = 1$. In this case, the oscillator and molecular orbital pair descriptions coincide. In a correlated electronic structure, each mode becomes a linear combination (that is, a wavepacket) of orbital pairs as represented by Eq. (5), and P^ν increases. P^ν is thus a useful measure of electronic correlations. The values of P^ν given in Fig.6B show that the higher oscillators are more collective and contain gradually increasing number of electron-hole pair states. The oscillators III and V corresponding to $d \rightarrow l^\star$ transitions have the most collective character. Such strongly correlated excitations require an extensive configuration-interaction calculations in an eigenstates approach. Here they appear naturally through the modes. The CEO is most attractive when P^ν is large because in a very efficient way it lumps the important effects of correlations directly into the observables. The collective nature of optical excitations at different frequencies can be analyzed

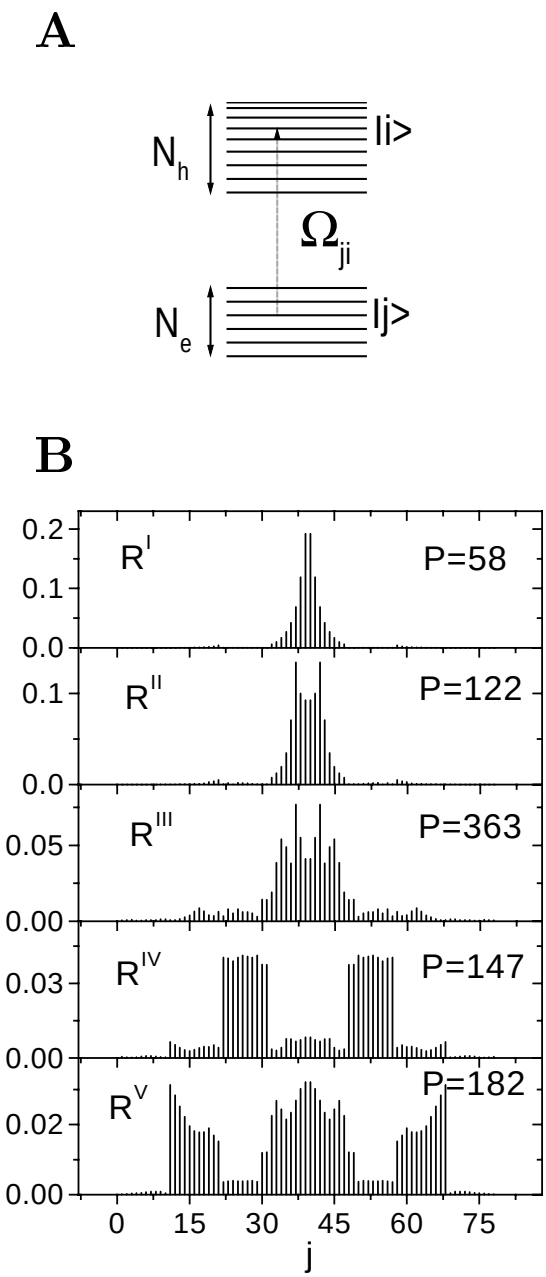

FIG. 6. (**A**) Origin of the collective electronic oscillators. Each transition between an occupaid and an unoccupied orbital represents an electron-hole oscillator. In a molecule with N_e occupied (electron) and N_h unoccupied (hole) orbitals we have altogether $N_e \times N_h$ oscillators. For a system with a filled valence and empty conduction band described by a "minimal basis set" $N_e = N_h = N/2$ and the number of oscillators is $N^2/4$. The collective oscillators Q_ν can be represented as superpositions of the electron-hole oscillators (see Eq. (6)). The participation ratio P^ν measures the effective number of electron-hole pairs contributing to a given collective oscillator. (**B**) The molecular orbital contributions and the inverse participation ratios of orbital pairs corresponding to the five dominant modes of PPV(10) absorption.

by expanding the induced density matrix in molecular orbitals $\delta\rho(\omega) = \sum_{i,j}^{N^2/4} \alpha_{i,j}(\omega)(c_i^+ c_j + c_j^+ c_i)$. we can then define a frequency – dependent participation ratio $P(\omega)$ by replacing $\alpha_{i,j}^\nu$ with $\alpha_{i,j}(\omega)$ in Eq.(6). (A normalization $\sum_{i,j} |\alpha_{i,j}(\omega)| = 1$ is assumed). $P(\omega)$ displayed in Fig.2B is a weighted average of the participation ratios P^ν of the contributing electronic oscillators.

We have used the molecular orbital representation to analyze the nature of mode III. In Fig. 4C we display its coordinate in the molecular orbital representation. The Figure clearly shows that only few molecular orbitals close to HOMO-LUMO contribute to this transition. The strongest orbitals can be identified as either delocalized or localized and mode III corresponds to $l \rightarrow d^\star$ and $d \rightarrow l^\star$ transitions. Our calculations further show that the frequencies of modes I, II, III are red-shifted and gradually saturate with increasing chain length, whereas the frequencies of modes IV and V are not affected by size. These findings are consistent with the delocalized and localized nature of the two groups of modes respectively as displayed in Figs.4 and 5.

Discussion and other Applications

The main reason for the success of the CEO representation can be rationalized as follows: An optical excitation moves an electron from some occupied to unoccupied orbitals, thereby creating an electron-hole pair. The natural description of the optical response should therefore be based on following the simultaneous and coupled dynamics of this pair; the two indices of the density matrix carry precisely this information. Molecular eigenstates, however, use a single-particle basis set. Correlations are incorporated through an extensive CI calculation. By working in a space of higher dimensionality (the pair) we capture the essential physics of the system, and even the simplest (TDHF) factorization yields an adequate description. In a single-particle basis, a much more extensive numerical effort is needed. A real space analysis of linear absorption which pinpoints the origin of each optical transition is obtained by displaying the electronic mode matrices graphically. The fact that only a few oscillators typically dominate the response greatly simplifies the theoretical description. The weak anharmonicities which justify the harmonic picture may be attributed to the large delocalization size. In atoms on the other hand collective excitations have been found to converge to local modes rather than to normal modes [30]. In semiconductors, the electron-hole pairs are loosely bound and form Wannier excitons [3]. In molecular aggregates, each pair is tightly bound and can be considered as a single particle (Frenkel exciton) [31,32]. Conjugated polymers are intermediate between these two extremes, and the collective oscillators in conjugated polymers can be viewed as charge-transfer excitons. The CEO thus offers a unified

description of different materials and allows a direct comparison of their optical properties [33]. Also, one can go beyond the PPP Hamiltonian and the TDHF approximation and include additional variables and use a different ansatz for the wave function [34]. Technically the calculation of optical properties using summation over states is also unified and universal. However, very different approximate schemes and terminologies are usually used in the calculation of the eigenstates of various systems; This prohibits a clear comparison and obscures the origin of differences. The electronic oscillator picture applies to all materials by simply changing parameters (such as the electron hole mass, the Coulomb interaction, and the hopping matrix elements) [35].

We next review the computational advantages of the electronic oscillator approach. The sum-only states method becomes rapidly more complex with molecular size. Both calculating the eigenstates and performing the necessary summations over them are intractable for large systems. Knowing the complete set of eigenstates allows the calculation of any optical response including to strong fields. This is therefore an "all or nothing" approach. The oscillator approach, carries less information but for considerably less effort. Computational time of CI calculations scales as N^6; The CEO procedure scales only as N^2. Our results allow the interpretation of the most interesting crossover region towards the bulk.

The significance of the oscillator picture is even more pronounced when nonlinear optical properties are calculated [4,5]. Interference effects in the sum-over-states approach result in an almost complete cancellation of large positive and negative contributions to optical susceptibilities [36,37], which limits the accuracy and makes approximate calculations dangerous (since innocent approximations may lead to huge errors). One consequence of this is that individual terms do not have the correct scaling with size. The latter is only obtained once all of the terms are carefully combined. In the oscillator picture these cancellations are built in from the start and each separate contribution to the susceptibility scales properly. The present discussion focuses on the resonant response. However, the real–space approach has been shown to provide an adequate description of the scaling and saturation of off-resonant linear and nonlinear polarizabilities [4,5].

We further note that by treating the electronic degrees of freedom as oscillators we can couple them more naturally to nuclear degrees of freedom, which constitute another set of oscillators. The incorporation of nuclear notions thus becomes much more straightforward compared with the eigenstate representation, and lends itself more easily to semiclassical approximations.

The oscillator approach allows us to develop a natural framework for the interpretation and the design of molecules with specific properties. Instead of asking which of the many-electron states are most relevant, we can explore how do different regions of the molecule couple and affect each other. We can translate $\delta\rho(t)$ into nonlocal response function $\alpha_{nm}(t)$, which shows how does the interaction with a field at point n affect the polarization at point m [38]. The total polarizability is given by summing this quantity over n and m $\alpha(t) = \sum_{nm} \alpha_{nm}(t)$. The nonlocal character of the response is intimately connected with the electronic coherence of the induced density matrix. One can then address directly the effects of donor-acceptor substitutions and geometry.

Electronic motions may now be probed directly on the femtosecond timescale and the nanometer lengthscale using nonlinear spectroscopic techniques. This has been recently demonstrated in semiconductor quantum wells [39], single molecule spectroscopy [40–42], and Rydberg atoms [43]. The CEO approach should allow us to analyze the temporal and spatial microscopic dynamics underlying energy and electron transfer processes in substituted conjugated molecules by using real-space wavepackets representing the single-electron density matrix. A physical picture for coherent versus incoherent electron transfer processes can then be developed in terms of off-diagonal or diagonal pathways respectively, of the electronic density matrix.

The CEO is conceptually similar to density functional theory which aims at calculating the ground state with an energy functional that only depends on the charge density that is, the diagonal elements of the density matrix in a localized basis [44]. The CEO is a natural extension of density functional theory to include the electronic coherences contained in off-diagonal elements. These carry the key information about electronic excitations and allow the calculation of spectra using only ground-state information.

[1] G. Herzberg, *Electronic Spectra of Polyatomic Molecules* (Van Nostrand, Toronto, 1966).

[2] J. F. Ward, *Rev. Mod. Phys.*, **37**, 1, (1965); B. J. Orr, J. F. Ward, *Mol. Phys.*, **20**, 513, (1971).

[3] H. Haug and S. W. Koch, *Quantum Chemistry of the Optical and Electronic Properties of Semiconductors*, (World Scientific, Singapore, 1990).

[4] S.Mukamel, A.Takahashi, H.X.Wang, G.Chen, *Science*, **266**, 251 (1994); V. Chernyak, S. Mukamel, *J.Chem.Phys.* **104**, 444 (1996);

[5] S. Tretiak, V. Chernyak and S. Mukamel, *Chem.Phys.Lett.* **259**, 55 (1996);

[6] T. Wagersreiter and S. Mukamel, *J. Chem. Phys.* , **104**, 7086 (1996).

[7] H. A. Lorentz, *The Theory of Electrons*, (Dover, New York, 1952); L. Rosenfeld, *Theory of Electrons*, (North-Holland, Amsterdam, 1951).

[8] U. Fano, *Rev. Mod. Phys.*, **45**, 553, (1974).

[9] E. B. Wilson, J. C. Decius, and P. C. Cross, *Molecular Vibrations*, (McGraw-Hill: New York, 1955).

[10] R. W. Hellwarth, *Progr. Quant. Electron.*, **5**, 2, (1977); G. Placzek, *The Rayleigh and Raman Scattering* (1934),

UCRL Transl. 256(L) (Washington, D.C.: U.S. Depertment of Commerce, 1962).
[11] S. Mukamel and H. X. Wang, *Phys.Rev.Lett.*, **69**, 65 (1992).
[12] H. Fukutome, *J. Mol. Struct. (Theochem)* **188**, 337 (1989), and references therein.
[13] R.McWeeny and B.T.Sutcliffe, *Methods of Molecular Quantum Mechanics* (Academic Press, New York, 1976); E. R. Davidson, *Reduced Density Matrices in Quantum Chemistry* (Academic Press: New York, 1976); A. Szabo, N. A. Ostlund, *Modern Quantum Chemistry* (McGraw-Hill: New York, 1989).
[14] R. S. Milliken, *J.Chem.Phys.*, **23**, 1833, 1841, 2338, 2343, (1955).
[15] D. Chandler, *Introduction to Modern Statistical Mechanics* (Oxford University Press, 1987).
[16] P. O. Lowdin, *Phys. Rev.* **97**, 1474, (1955); *Adv. in Phys.* **5**, 1, (1956).
[17] A. E. Reed, L. A. Curtiss, and F. Weinhold, *Chem. Rev.*, **88**, 899, (1988); A. E. Reed, R. B. Weinstock, and F. Weinhold, *J. Chem. Phys.*, **83**, 735, (1985).
[18] P.Ring and P.Schuck, *The Nuclear Many-Body Problem* (Springer-Verlag, New York, 1976).
[19] S. Tretiak, V. Chernyak, and S. Mukamel, *Phys. Rev. Lett.* **77**, 4656 (1996).
[20] T.W.Hagler, K.Pakbaz, K.F.Voss, and A.J.Heeger, *Phys.Rev.B.* **44**, 8652 (1991).
[21] D.D.C.Bradly, R.H.Friend, H.Lindenberger, and S.Roth, *Polymer* **27**, 1709 (1986); D. A. Halliday, P. L. Burn, R. N. Friend, D.D.C.Bradly, A. B. Holmes, and A. Kraft Synthetic Metals, **55-57**, 954, (1993).
[22] A.Sakamoto,Y.Furukawa, and M.Tasumi, *J.Chem.Phys.* **96**, 1490 (1992); *ibid.* **96**, 3870 (1992).
[23] B.Tian,G.Zerbi,R.Schenk,K.Müllen, *J.Chem.Phys.* **95**, 3191 (1991); *ibd.* B.Tian, G.Zerbi, and K.Müllen, **95**, 3198 (1991).
[24] U.Rauscher, H.Bässler, D.D.C.Bradley, and M.Hennecke, *Phys.Rev.B.* **42**, 9830 (1990).
[25] J.L.Bredas, R.R.Chance, R.H.Baughman, and R.Silbey, *J.Chem.Phys.* **76**, 3673 (1982).
[26] J.Cornil, D.Beljonne, R.H.Friend, J.L.Bredas, *Chem.Phys.Lett.* **223**, 82 (1994).
[27] W. Z. Wang, A. Saxena, and A. R. Bishop, *Phys. Rev. B* **50**, 6068 (1994).
[28] M. Chandross, S. Mazumdar, S. Jeglinski, X. Wei, Z. V. Vardeny, E. W. Kwock and T. M. Miller *Phys. Rev. B*, **50**, 14702 (1994).
[29] A. K. Ghosh, D. L. Morel, T. Feng, R. F. Shaw, C. R. Rowe, *J. Appl. Phys.*, **45**, 230, (1974).
[30] R. S. Berry in *Structure and Dynamics of Atoms and Molecules: Conceptual Trends*, edited by J. L. Calais and E. S. Kryachko (Kluwer Academic Publishers, 1995), pp. 155-181.
[31] F.F. So and S.R. Forrest, *Phys. Rev. Lett.*, **66**, 2649 (1991); E.I. Haskal, Z. Shen, P.E. Burrows, and S.R. Forrest, *Phys. Rev. B*, **51**, 4449 (1995).
[32] R. van Grondelle, J. P. Dekker, T. Gillboro, and V. Sundström, *Biochim. Biophys. Acta*, **1187**, 1, (1994); S. E. Bradforth, R. Jimenez, F. von Mourik, R. van Grondelle, and G. R. Fleming, *J.Phys.Chem.*, **99**, 16179, (1995).
[33] B.I. Greene, J. Orenstein, S. Schmitt - Rink, *Science*, **247**, 679 (1990).
[34] V. M. Axt and S. Mukamel *Rev. Mod. Phys.* (in press).
[35] S. Yokojima, T. Meier, and S. Mukamel *J. Chem. Phys.*, **106**, 3837, (1997).
[36] S.Mukamel, *Principles of Nonlinear Optical Spectroscopy* (Oxford, New York, 1995).
[37] D.C. Rodenberger, J. F. Heflin, A. F. Garito, *Phys.Rev.A*, **51**, 3234 (1995); D. C. Rodenberger and A. F. Garito, *Nature*, **359**, 309 (1992).
[38] Th. Wagersreiter and S. Mukamel, *J. Chem. Phys.* , **105**, 7995 (1996).
[39] S. Weiss, M.-A. Mycek, J.-Y. bigot, S. Schmitt-Rink, and D.S. Chemla, *Phys. Rev. Lett.* **69**, 2685 (1992).
[40] X. S. Xie and R. C. Dunn, *Science* **265**, 361 (1994).
[41] W. P. Ambrose, P. M. Goodwin, J. C. Martin, and R. A. Keller, *Science* **265**, 364 (1994).
[42] J. K. Trautman, J. J. Macklin, L. E. Brus, and E. Betzig, *Nature* **369**, 40 (1994).
[43] J. A. Yeazell and C. R. Stroud *Phys. Rev. A* **43**, 5153 (1991).
[44] R. G. Parr and W. Yang, *Density-Functional Theory of atoms and Molecules*, (Oxford University Press, New York, 1989).

ACKNOWLEDGMENTS

The support of the Air Force Office of Scientific Research and the National Science Foundation (NSF) is gratefully acknowledged. Th. W. gratefully acknowledges the support of the Fonds zur Förderung der Wissenschaftlichen Forschung, Austria, in form of an E.Schrödinger Stipendium (grant no. J-01023-PHY). The calculations were conducted using the resources of the Cornell Theory Center, which receives major funding from the NSF and New York State.